

A Modular and Cost-Effective Superconducting Generator Design for Offshore Wind Turbines

Ozan Keysan, Markus Mueller

Institute for Energy Systems, University of Edinburgh, EH93JL, UK

E-mail: o.keysan@ed.ac.uk

Abstract.

Superconducting generators have the potential to reduce the tower head mass for large(10 MW) offshore wind turbines. However, a HTS generator should be as reliable as conventional generators for a successful entry to the market. Most of the proposed designs use the superconducting synchronous generator concept, which has a higher cost than conventional generators and suffer from reliability issues. In this paper, a novel claw-pole type superconducting machine is presented. The design has a stationary superconducting field winding, which simplifies the design and increases reliability. The machine can be operated in independent modules, thus even one of the sections fails the rest can operate at until next maintenance. Another advantage of the design is very low superconducting wire requirement; a 10 MW 10 rpm design is presented which uses 13 km of MgB2 wire at 30 K. The outer diameter of the machine is 6.5 m and weighs 184 tonnes including the structural mass. The design thought to be a good candidate to enter the renewable energy market with its low cost and robust structure.

1. Introduction

Average size of offshore wind turbines was 2 MW a decade ago, but now increased to 5 MW [1]. The installation and maintenance cost of large offshore wind turbines are cheaper per MW compared to smaller wind turbines, and it takes less time to build a wind farm with larger turbines, which all help to reduce the cost of energy [2]. It is aimed to build 10 MW, and even 20 MW, wind turbines [3], however, the tower head mass of larger wind turbines, which is estimated as 760 t for a 10 MW turbine, becomes a critical issue [3].

Direct-drive superconducting machines are proposed to minimize the tower head-mass and increase the energy yield [4, 5, 6]. It is stated in [5] that a 6 MW HTS direct drive generator may have 50 % of the mass of a direct drive PM generator and the lower mass of generator may enable transport and installation of the turbine in one piece. In order to compare mass to torque ratio of HTS machines with other type of generators, data from direct-drive systems have been collected and the results are presented in a bubble chart in Figure 1 and tabulated in Table 1. Although, some designs are just conceptual designs and some are commercial products, the graph provides a good understanding of torque density capability of HTS machines. The dashed line represents ratio of generator mass to torque for permanent-magnet machines which is estimated as 25 kg/kNm by Bang *et al.* in [2]. The continuous line represents the linear trend line estimated using the HTS machines in the graph. From the graph, it is clear that HTS machines are lighter than PM generators for applications with torque requirements larger than 3000 kNm. The equation of the trend line can be represented as:

$$Mass(t) = 0.011 \times Torque(kNm) + 45 \quad (1)$$

Although, superconducting machines are lighter than conventional generators (e.g. geared doubly-fed induction generators or direct-drive permanent magnet generators), low-mass is not the only desired property for offshore wind turbines. Firstly, offshore wind turbine generators operate in harsh conditions and are exposed significant vibration levels in the nacelle. Secondly, maintenance of offshore wind turbines are expensive and any failures result in long down periods adding lost generation income on top of the repair cost. Therefore, reliability and serviceability are very important for offshore wind turbines and in order to penetrate into the offshore renewable energy market, the superconducting generators should be as reliable and easy to maintain as the conventional generators. Compared to conventional generators superconducting generators have the disadvantage of having extra subsystems such as cryocooler, vacuum system etc. Therefore, any critical system should have redundancy to get fail-safe operation. It is desirable to have modularity in the power take-off system to make transportation, installation and maintenance easier.

The most common superconducting machine topology is the synchronous superconducting machine [20, 21], which has a copper armature winding and a rotating DC-excited superconducting field winding, however, it may not be the most suitable

Table 1: Torque density comparison conventional and superconducting generators.

| | Manufacturer | Power (MW) | Speed (rpm) | Mass (t) | Torque (kNm) | Mass/T (kg/kNm) | Type |
|----|-------------------------|---------------|----------------|-------------|-----------------|--------------------|--------|
| 1 | Harakosan [7] | 1.5 | 18 | 47.2 | 796 | 59.3 | PMG |
| 2 | The Switch [7] | 3.8 | 21 | 81 | 1728 | 46.9 | PMG |
| 3 | NewGen [8] | 4 | 19 | 36.4 | 2010 | 18.1 | PMG |
| 4 | NREL-AMSC [9] | 3.1 | 12.5 | 90 | 2368 | 38.0 | PMG* |
| 5 | Bang et. al. [10] | 5 | 12 | 90.8 | 3979 | 22.8 | TFPM |
| 6 | | 5 | 12 | 60.5 | 3979 | 15.2 | TFPM* |
| 7 | NTNU Reference [11] | 10 | 13 | 260 | 7346 | 35.4 | PMG |
| 8 | NREL-AMSC [9] | 6 | 12.3 | 177 | 4658 | 38.0 | PMG* |
| 9 | | 10 | 11.5 | 315 | 8304 | 37.9 | PMG* |
| 10 | Bang et. al. [2] | 10 | 10 | 325 | 9549 | 34.0 | PMG * |
| 11 | Enercon-E126 | 7.5 | 12 | 220 | 6031 | 36.4 | EESM |
| 12 | Lee et. al. [12] | 5 | 230 | 44 | 208 | 212.0 | HTSG* |
| 13 | | 5 | 230 | 18 | 208 | 86.7 | HTSG* |
| 14 | Maki [13] | 2 | 21.5 | 54 | 888 | 60.8 | HTSG |
| 15 | NREL-AMSC [9] | 3.1 | 12.5 | 76 | 2368 | 32.1 | HTSG |
| 16 | AMSC [14] | 36.5 | 120 | 75 | 2905 | 25.8 | HTSG |
| 17 | Maki [13] | 5 | 14.8 | 108 | 3226 | 33.5 | HTSG |
| 18 | NREL-AMSC [9] | 6 | 12.3 | 97 | 4658 | 20.8 | HTSG |
| 19 | Maki [13] | 8 | 12 | 154 | 6366 | 24.2 | HTSG |
| 20 | Converteam [5] | 8 | 12 | 100 | 6366 | 15.7 | HTSG |
| 21 | NREL-AMSC [9] | 10 | 11.5 | 160 | 8303 | 19.3 | HTSG |
| 22 | AMSC [15] | 10 | 11 | 150 | 8681 | 17.3 | HTSG |
| 23 | Abrahamsen et. al. [16] | 10 | 10.4 | 88 | 9182 | 9.6 | HTSG * |
| 24 | General Electric [17] | 10 | 10 | 143 | 9549 | 15.0 | HTSG * |
| 25 | AML [18] | 10 | 10 | 70 | 9549 | 7.3 | HTSG * |
| 26 | Sung et. al. [19] | 10 | 10 | 147 | 9549 | 15.4 | HTSG * |
| 27 | | 10 | 10 | 196 | 9549 | 20.5 | HTSG * |

*The machine is not optimised for minimum mass.

*Ring-shaped TFPM.

*The machine is not optimised for minimum mass.

*The diameter is limited to 4.3 m.

*Estimated mass.

*Homopolar superconducting machine.

*Air-cored superconducting synchronous machine.

*The machine is found to be economically infeasible.

*The generator actually uses NbTi low temperature superconductor wire.

*Fully superconducting generator with MgB2 wires.

*With YBCO wire.

*With Bi-2223 wire.

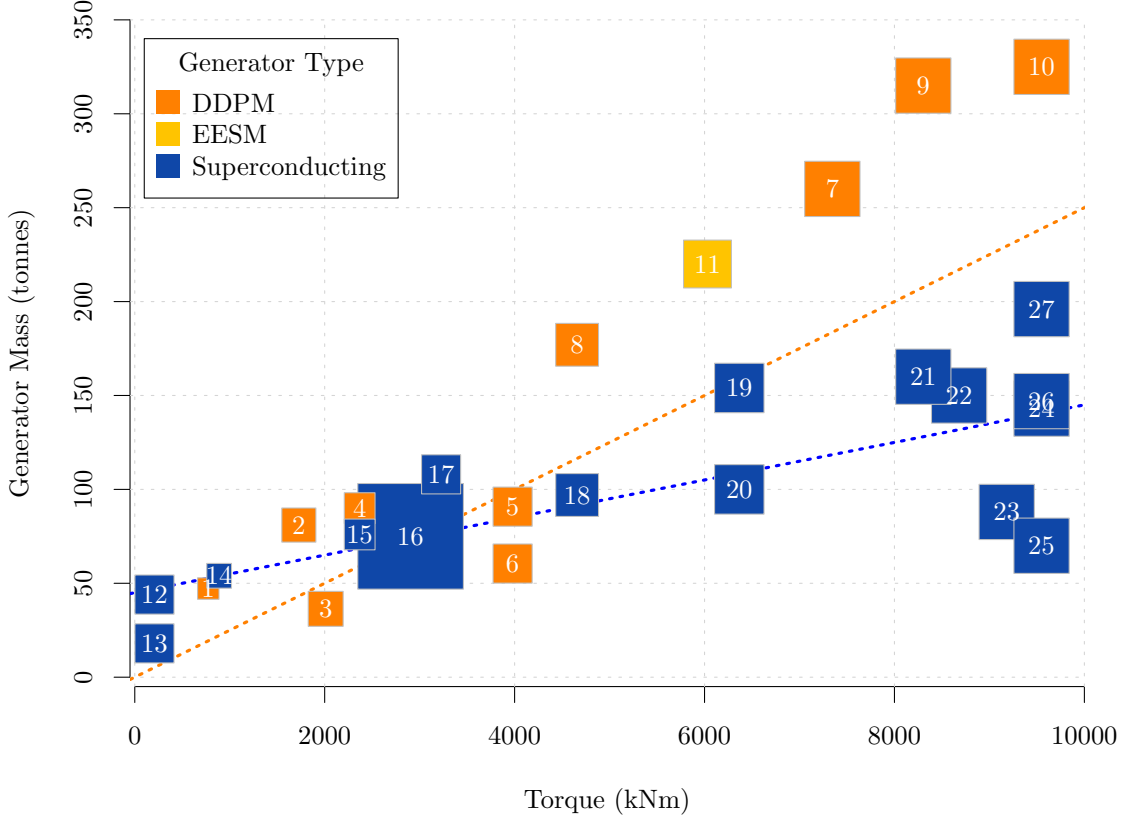


Figure 1: Mass of different large direct-drive machines as a function of the torque, area of the square represents the power rating. DDPM: Direct drive permanent magnet generator, EESM: Electrically excited synchronous machine, Superconducting: High-temperature superconducting generator. Orange line represents generator mass to torque ratio (m/T) of 25 kg/kNm for permanent-magnet machines as given in [2]. Blue line is the linear trend line for the superconducting machines.

topology for an offshore wind turbine application. The synchronous generator with a superconducting rotor has the following problems and challenges:

- **Rotating Transfer Coupler:** In a rotating superconducting coil configuration, rotating transfer coupler introduces reliability issues and requires regular maintenance. Furthermore, it is the single point of failure for the whole generator system. Electric excitation system has the same problem.
- **Torque Transfer Structure:** Machines with rotating field superconducting winding require a torque transfer structure that is thermally insulating and structurally sound, which is difficult to design and expensive to manufacture.
- **Transient forces in the SC coil:** Second generation HTS tapes are prone to high stresses and bending. They are exposed to centrifugal and other transient forces in a rotating superconducting winding design.
- **Superconducting Wire Usage:** In a conventional synchronous superconducting machine, the magnetic flux has to cross the air-gap, vacuum and insulation layers.

Thus, the equivalent magnetic gap is larger than the mechanical gap, which increases the superconducting coil requirement.

There are novel machine designs in literature aim to overcome some of these problems. AMSC plans to put the cold heads in the rotor for their 10 MW, 10 rpm generator design [22], but the design still requires cryocouplers. General Electric eliminated cryocouplers using a stationary superconducting coil and a rotating copper armature configuration [23]. In [24], a superconducting generator with stationary superconducting armature and field windings are shown, the machine is similar to a switched reluctance machine.

2. Double Sided Claw Pole Concept

In [25, 26] a radial flux claw pole machine is presented. The novelty of the design lays in having a single stationary superconducting field winding, which simplifies the cooling system. The rotor just consists of modular claw poles, which can be easily disassembled if required. In this paper, the radial flux claw pole machine is modified as shown in Figure 2.

The advantages of the double-sided claw pole topology compared to other superconducting machine designs can be listed as:

- The machine has a stationary superconducting field winding, which means: no cryocoupler, no brushes or brushless exciters, no vibrational or rotational forces acting on the SC coil.
- The magnetic attraction forces on the rotor structure are symmetrical and cancel each other, which means reduced structural mass.
- The machine has two armature windings that can be operated independently. Thus, the modularity is increased.
- The machine uses significantly less superconducting coil due to iron-cored structure and loop-shaped field winding.

The machine analysed using 3D finite-element software and the flux density vectors in the machine are presented in Figure 3. The flux density vectors shown in Figure 3c verify the operation of the proposed topology, as the magnetic flux created by the superconducting coil links both armature cores through the claw poles as depicted in Figure 2d.

2.1. Material Selection

Power density of the machine is limited by magnetic saturation as it is iron-cored, which makes the material selection very critical. Vacuumschmelze introduced a cobalt-iron alloy called VacoFlux50, which can be manufactured in laminations and has an impressive magnetic saturation limit with 2.35 T at 16 kA/m [27]. This material is

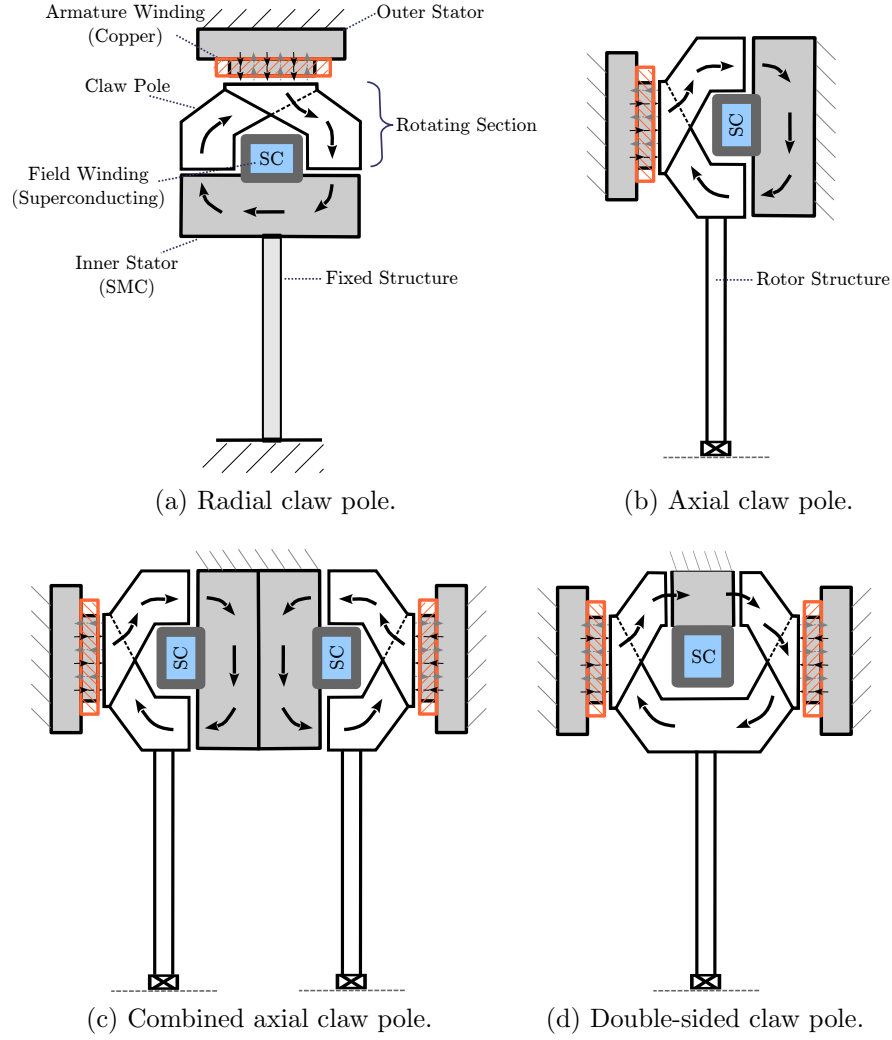


Figure 2: Evolution of the claw pole topology.

promising for superconducting machine designs with its high saturation limit and used in the calculations in this paper.

2.2. Sectioned Cryostat

Although, the initial design has a single loop-shaped superconducting field winding, it is difficult to manufacture and install the field winding in one piece in multi-MW scale. In the original design, the cryostat is fixed to the inner surface of the field core as shown in Figure 4a, however, it is also possible to mount another coil on the outer surface of the field core as in Figure 4b. Then, the cryostat can be divided into smaller sections as shown in Figure 4c. This configuration has two main advantages. Firstly, it is easier to manufacture and install the sectioned cryostat compared to full span cryostat. Secondly, two independent cryostat introduces modularity to the system, thus even one of the cryostats fails the machine can still operate at half-capacity until maintenance.

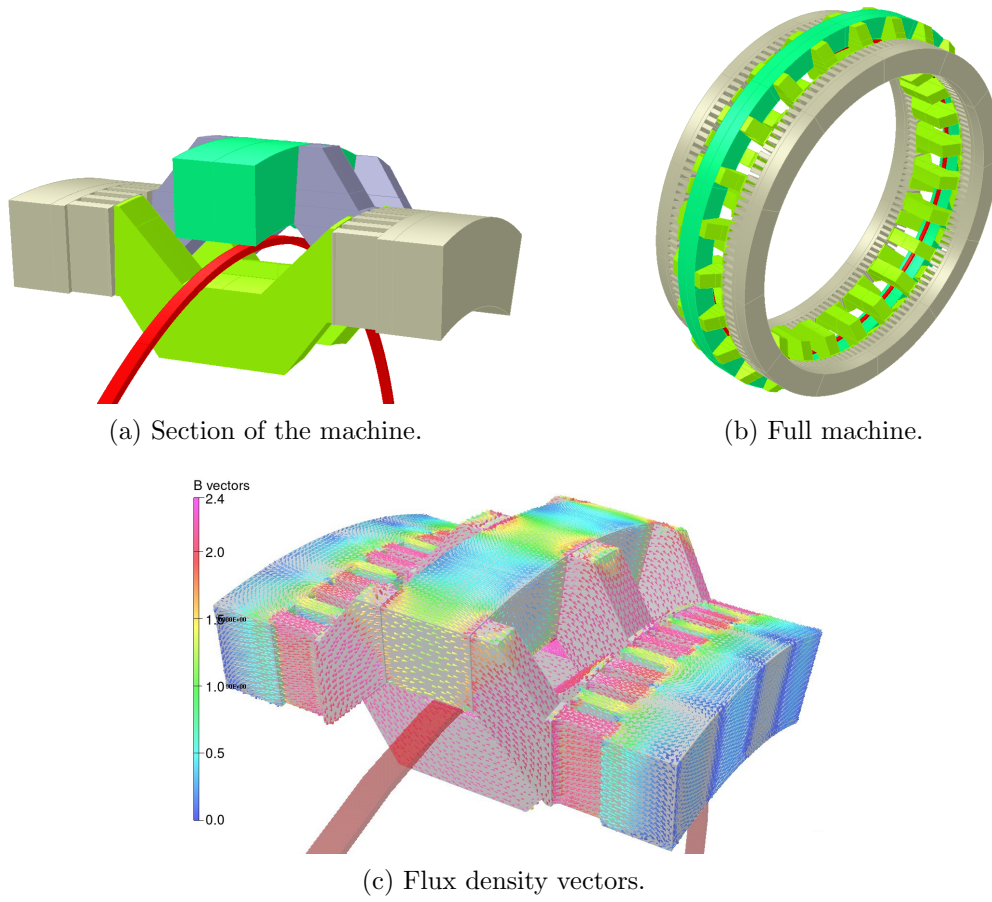


Figure 3: The double-claw pole machine model and flux density vectors.

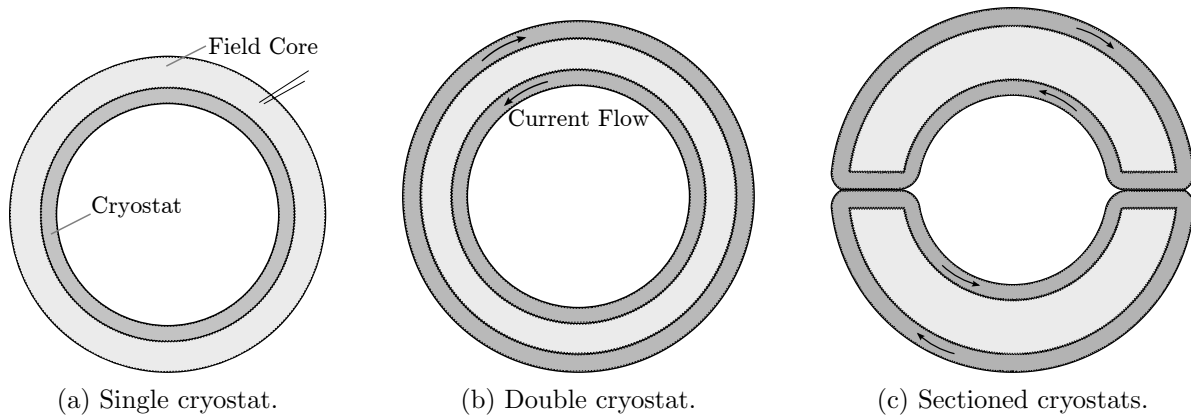


Figure 4: Sectioned cryostat design for the double-claw pole machine.

| | |
|------------------------|----------------------|
| Power Rating | 10 MW |
| Rotational Speed | 10 rpm |
| Number of Poles | 88 |
| Outer Diameter | 6.63 m |
| Armature Diameter | 5.84 m |
| Rotor Radius | 3.20 m |
| Inner Radius | 2.29 m |
| Axial Length | 1.38 m |
| Number of Stator Slots | 66 |
| Number of Turns | 96 |
| Induced Coil Voltage | 173 V _{rms} |
| Phase Voltage | 3.3 kV _{ll} |

Table 2: Main specifications of the optimized 10 MW, 10 rpm design.

3. Design of a 10 MW Superconducting Generator

As presented in the introduction section and in Table 1, 10 MW, 10 rpm superconducting generator designs are quite common in the literature, therefore, a 10 MW double-sided claw pole machine is designed for a better comparison with other superconducting machine designs.

A parametrized FEA model of the proposed topology is developed, which estimates the air gap flux density and power output. The machine is optimized using the genetic algorithm optimization tool “rgenoud” [28]. The objective function is defined as the total active material mass, with pre-defined constraints in outer diameter, phase voltage and current density.

The main specifications of the optimum design is presented in 2 and the outline is shown in 5. The machine has an outer diameter of 6.6 m and an axial length of 1.4 m, which is a similar size to a 5 MW direct-drive permanent magnet generator. The machine has an electrical frequency of 7.33 Hz. There are 11 coils in series and two parallel branches for each phase.

Figure 6 shows the flux density distribution in the stator tooth when the large claw pole and small claw pole are aligned with the middle stator tooth.

3.1. Mass Estimation

The excess structural mass in the large direct-drive generators is a serious issue. Although, the proposed machine has a smaller diameter than equivalent DDPM generators, which helps to reduce the structural mass, the high air-gap flux density increases the stress on the mechanical structure.

It is possible to install the proposed generator in two different configurations as shown in Figure 7: axial armature winding or radial armature winding. In this paper,

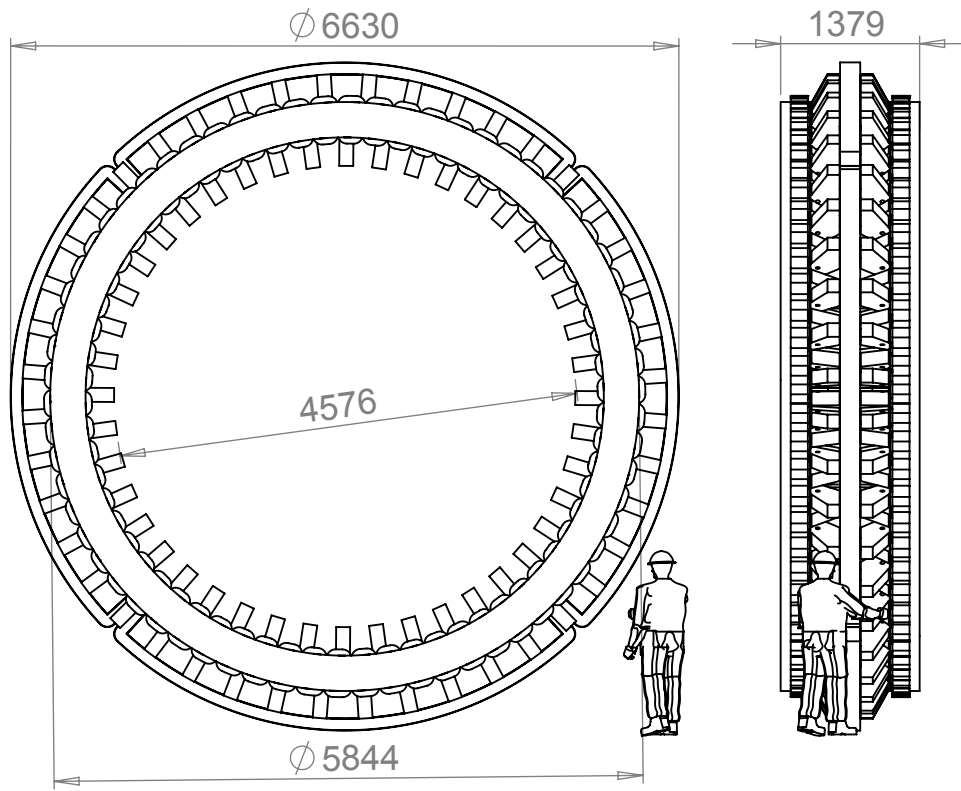
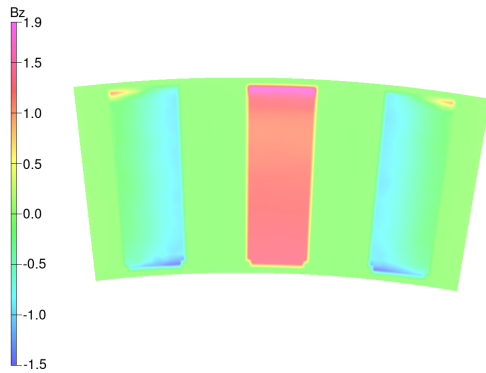
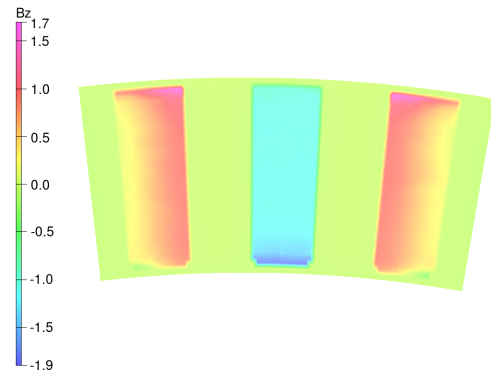


Figure 5: The outline dimensions of the 10 MW, 10 rpm generator design. Dimensions are in mm.



(a) Middle tooth aligned with the large claw pole.



(b) Middle tooth aligned with the small claw pole.

Figure 6: Flux density distribution in Z direction (into the page) in the stator teeth at mean coil radius.

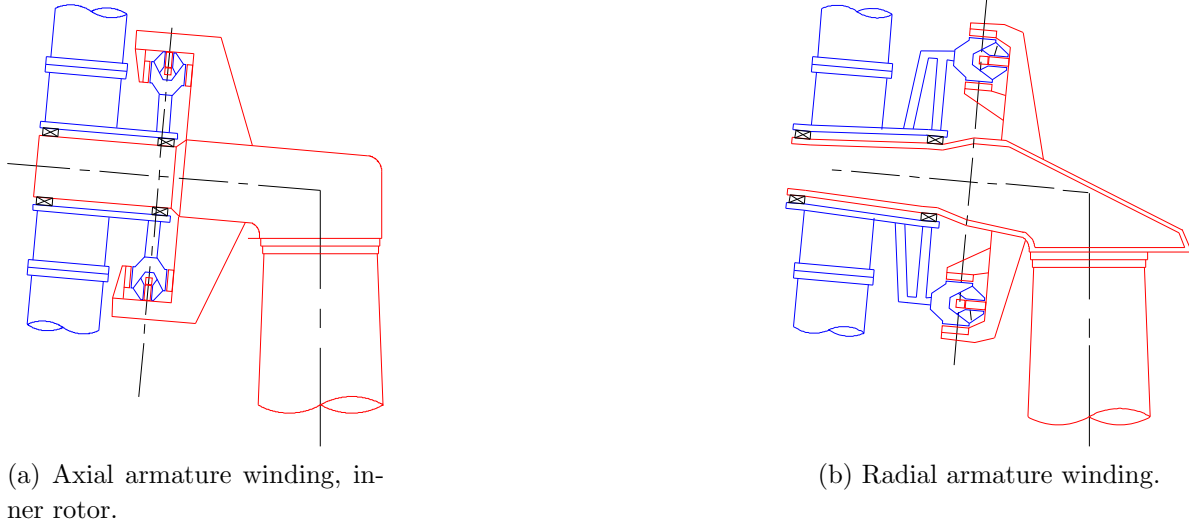


Figure 7: Two possible configurations for the installation of double-claw pole machine to a wind turbine (Drawings modified from [29]).

| | |
|---------------------|---------|
| Small Claw Pole | 114 kg |
| Large Claw Pole | 314 kg |
| Rotor Structure | 42.8 t |
| Stator Structure | 83.5 t |
| Magnetic Core | 52.4 t |
| Copper | 2.3 t |
| Cooling - Cryostats | 3.2 t |
| Total Mass | 184.2 t |

Table 3: The structural and active material mass estimations for the 10 MW, 10 rpm machine.

axial armature configuration is used for mass calculations, which are presented in Table 3. The total mass of the generator is estimated as 184 tonnes. The structural mass dominates the total mass by 68 %.

3.2. Estimation of Losses

Main losses in the machine are presented in 4. Copper armature winding dissipates 510 kW of heat loss, which is cooled down by 40 kW of air blowers. Core losses in the machine are quite low due to an electrical frequency of 7.3 Hz.

It is important to accurately estimate the heat leakage in the cryostats, which can be divided into gas heat conduction through the vacuum, radiation heat from warm walls of the cryostat, conduction through superconducting coil mechanical support, heat leakage through current leads and eddy current loss. These losses are estimated using

| | |
|------------------------|--------|
| Copper Loss | 510 kW |
| Core Loss | 7 kW |
| Cryocoolers | 24 kW |
| Air Blowers (Armature) | 40 kW |
| Efficiency | 94.5 % |

Table 4: Main losses and efficiency estimation for the 10 MW, 10 rpm design.

the methodology presented in [30, 31].

The surface area of a single cryostat is 6.1 m^2 , which gives the total cryostat wall area as 24.4 m^2 . The cryostat used in the proposed generator is different to a superconducting rotor, where a cylindrical cryostat is used. Assuming a 5 m diameter, surface area of a cylindrical cryostat can be calculated as 55 m^2 , which is twice the area of the proposed cryostat. Thus, the heat loss through cryostat wall is lower.

The heat loss can be calculated as shown in [32]. The operating pressure is chosen as 10^{-3} Pa , which can be achieved using standard industrial equipments. The heat loss at this vacuum level is 3.9 W. Radiation loss is calculated as 17.5 W by using 10 mm of MLI insulation, which has 30 layers.

Suspension straps are required to mechanically support the superconducting coil. As there are no electromagnetic torque acting on the superconducting coil, the design of these suspension straps relatively straightforward compared to the torque tubes of other types of superconducting machines. The distance between suspension straps is assumed as 1 m, which gives 10 straps per cryostat. Assuming the straps are made of G10-CR fibreglass, the conduction heat loss can be calculated as 13.5 W per cryostat.

The length of current leads should be carefully assessed as it depends on two factors: resistive losses and heat conduction through ambient. For minimum losses, the resistive and conductive losses should be equal as presented in [33]. Assuming a current input of 90 A, the heat loss in a single current lead is found as 5.9 W (11.8 W per cryostat).

Total heat losses in the cryostats are tabulated in Table 5. The heat loss at 65 K is also presented, which is estimated as 154.2 W. The total thermal budget of the machine at 30 K is 157.2 W, slightly larger than the heat loss at 65 K. Adding 25% safety margin, the machine can be cooled using 4 x 50 W cryocoolers. A suitable cooling system for such a requirement is selected as Cryomech's Gifford-McMahon AL230 cold-head coupled with CP950 compressor, which can supply 60 W of cooling power at 30 K [34]. Total cooling system mass in the generator is calculated as 2,000 kg with an electrical power input of 24 kW.

To summarize, the proposed topology has the advantage of independent cryostats, which increases the modularity and overall availability of the system. The total cryostat wall area is smaller compared to the conventional cylindrical cryostats, which helps to reduce the gas conduction and radiation losses. However, the sectioned cryostat results in higher number of current leads and suspension straps which increases the conduction

| | 30 K MgB2–90 A | 65 K YBCO–120 A |
|----------------------------------|-------------------|--------------------|
| Gas Conduction (at 10^{-3} Pa) | 3.9 W | 3.4 W |
| Suspension Straps | 54.0 W | 50.0 W |
| Radiation | 17.5 W | 17.4 W |
| Current leads | 47.2 W | 48.8 W |
| Cold-head sleeve | 15.6 W | 15.6 W |
| Eddy Current | 4.0 W | 4.0 W |
| Other | 15.0 W | 15.0 W |
| Total loss | 157.2 W | 154.2 W |

Table 5: Thermal budget for the 10 MW, 10 rpm design.

| | |
|----------------------|------------|
| Mean turn length | 10.4 m |
| MMF of the SC | 32.4 kAt |
| Number of Cryostats | 4 |
| Total SC requirement | 1348 kAt.m |

Table 6: Superconducting winding specifications for the 10 MW, 10 rpm design.

losses. In general, the heat loss is within the reasonable values. For example in [35], it is stated that six to ten CTI-1020 cryogenic coolers are used for AMSC’s 10 MW superconducting generator, provides 280–450 W of cooling power. In [23], the total cooling requirement for the GE’s 10 MW LTS superconducting generator is estimated as 131 W, and in [30], 500 W is defined as the upper limit of the cooling power for a 5 MW superconducting generator.

3.3. Superconducting Coil Requirements

The magneto-motive-force of the superconducting coil is selected by the optimisation algorithm as 32.4 kAt, which saturates the claw poles up to 2.3 T. Total superconducting coil requirement in four cryostats (4 x 10.4 m) can be calculated as 1348 kAt.m as shown in Table 6.

The required superconducting wire length is calculated for three cases: MgB2 at 30 K, YBCO at 30 K, YBCO at 65 K. In critical current calculations magnetic flux penetrating into the superconducting coil is taken into account. The results presented in Table 7 show the SC wire requirement is substantially less than other superconducting designs. In Table 8, SC wire requirements of several 10 MW designs are compared. In particular, air-cored topologies require hundreds of kilometres of superconducting wire. The closest design is the AMSC [35], which requires 36 km of YBCO at 30 K. However, the proposed design just requires 3.4 km of YBCO at that temperature, which is less than one tenth of the AMSC’s design.

| | MgB2 | YBCO | |
|---------------------------|---------|---------|---------|
| Operating Temperature | 30 K | 30 K | 65 K |
| Current ($0.8I_c$) | 90 A | 400 A | 100 A |
| Number of turns | 360 | 81 | 324 |
| Wire thickness | 0.67 mm | 0.22 mm | 0.22 mm |
| Wire width | 3.65 mm | 4.8 mm | 4.8 mm |
| Wire length(per cryostat) | 3744 m | 842 m | 3370 m |
| Wire length (total) | 15.0 km | 3.4 km | 13.5 km |

Table 7: Superconducting tape requirements for the 10 MW, 10 rpm design (MMF=32.4 kAt).

Table 8: Comparison of superconducting wire requirements and total mass of 10 MW direct-drive superconducting generators.

| | SC Wire Requirement | Total Mass |
|-----------------------------|--------------------------|------------|
| Proposed Design | 15 km MgB2 (30 K) | 184 t |
| | 3.4 km YBCO (30 K) | |
| | 13.5 km YBCO (65 K) | |
| Abrahamsen et. al. [16] | 200–300 km YBCO | 88 t |
| General Electric [17] | 720 km NbTi | 143 t |
| AMSC/Snitchler et. al. [35] | 36 km YBCO (30K) | 150 t |
| Sung et. al. [19] | 586 km YBCO | 147 t |
| Sung et. al. [19] | 222 km Bi2223 | 196 t |
| Terao et. al. [36] | 270 km HTS + 275 km MgB2 | - |
| Kim et. al. [37] | 919 km HTS | - |
| Quddes et. al. [38] | 1050–1400 km HTS | - |

The low SC requirement is due to two main reasons. Firstly, the coil is loop shaped, which results in better utilization of the MMF per length of the coil. Secondly, as shown in Figure 8, the magnetic gap in the claw pole topology equals to the mechanical gap. However, in a typical superconducting machine the flux has to pass through many layers (vacuum, radiation shield, EM shield, etc.) through the cryostat, which results in a much larger magnetic gap and increased MMF requirement.

4. Conclusion

This paper presents a novel superconducting machine design by introducing the stationary superconducting field winding concept. The concept simplifies the cryostat design by eliminating the transfer couplers and any rotating parts, which helps to increase the reliability. Furthermore, a sectioned cryostat concept is also presented. This improves modularity and redundancy to the system, which is critical for offshore

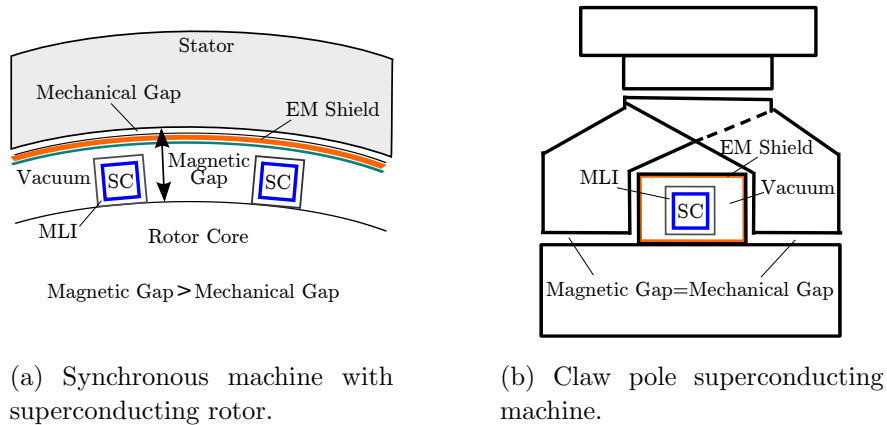


Figure 8: Magnetic and mechanical gap comparison for the typical superconducting machine and the claw pole machine.

wind turbines where the O&M is difficult and expensive.

Maybe the biggest advantage of the proposed topology is the minimal superconducting wire requirement. The 10 MW design requires 32.4 kAt, which is equal to 15 km of MgB2 at 30 K or 13.5 km of YBCO at 65 K. This is substantially less than other superconducting designs.

It may be argued that the power density of the machine is limited because of the iron-cored structure and it is heavier than its competitors. Although, it is true that the proposed design is 23 % higher than the trend-line of superconducting machines, it is still 40 % lighter than the similar rated DDPMGs.

Thus, it is believed that the proposed claw pole topology is a very suitable design to initiate the superconducting generators for offshore wind turbines. The first prototypes can be used to prove that superconducting generators are as reliable as alternative power take-off systems. It may be the intermediate step between conventional generators and more power dense fully-superconducting generators that will be built in future, when the price of superconducting wires come down.

References

- [1] BVG, "Offshore wind cost reduction pathways - Technology work stream," BVG Associates, Tech. Rep. May, 2012. [Online]. Available: http://www.thecrownestate.co.uk/media/305086/BVG_OWCRP_technology_work_stream.pdf
- [2] D. Bang, H. Polinder, G. Shrestha, and J. A. Ferreira, "Review of Generator Systems for Direct-Drive Wind Turbines," in *Proceedings of the 2008 European wind energy conference, EWEC-2008*, Brussels, 2008, pp. 1–10. [Online]. Available: <http://proceedings.ewea.org/ewec2008/>
- [3] "UpWind - Design Limits and Solutions for Very Large Wind Turbines - EU 6th Frame Project," Tech. Rep., 2011. [Online]. Available: www.upwind.eu
- [4] M. Lesser and J. Müller, "Superconductor Technology, Generating the Future of Offshore Wind Power," *Renewable Energy World Conference, Cologne, Germany*, pp. 1–10, 2009.
- [5] C. Lewis and J. Muller, "A Direct Drive Wind Turbine HTS Generator," *2007 IEEE Power Engineering Society General Meeting*, pp. 1–8, Jun. 2007.

- [6] S. Kalsi, K. Weeber, H. Takesue, C. Lewis, H. Neumueller, and R. Blaugher, "Development status of rotating machines employing superconducting field windings," *Proceedings of the IEEE*, vol. 92, no. 10, pp. 1688–1704, Oct. 2004. [Online]. Available: <http://ieeexplore.ieee.org/lpdocs/epic03/wrapper.htm?arnumber=1335557>
- [7] Y. Duan and R. G. Harley, "Present and future trends in wind turbine generator designs," *2009 IEEE Power Electronics and Machines in Wind Applications*, pp. 1–6, Jun. 2009. [Online]. Available: <http://ieeexplore.ieee.org/lpdocs/epic03/wrapper.htm?arnumber=5208401>
- [8] S. Engström, B. Hernnas, C. Parkegren, and S. Waernulf, "Development of NewGen - a New Type of Direct-Drive Generator," in *European Wind Energy Conference-EWEC*, vol. 4, no. 1, 2004, pp. 22–25. [Online]. Available: http://www.2004ewec.info/files/23_1400_staffanengstrom.01.pdf
- [9] B. Maples, M. Hand, and W. Musial, "Comparative Assessment of Direct Drive High Temperature Superconducting Generators in Multi-Megawatt Class Wind Turbines," National Renewable Energy Laboratory (NREL), Golden, CO., Tech. Rep. October, 2010. [Online]. Available: http://www.osti.gov/bridge/product.biblio.jsp?osti_id=991560
- [10] D. Bang, H. Polinder, G. Shrestha, and J. A. Ferreira, "Ring-shaped transverse flux PM generator for large direct-drive wind turbines," in *2009 International Conference on Power Electronics and Drive Systems (PEDS)*. IEEE, Nov. 2009, pp. 61–66. [Online]. Available: <http://ieeexplore.ieee.org/lpdocs/epic03/wrapper.htm?arnumber=5385933>
- [11] E. B. Smith, "Design Av Nacelle fro en 10 MW VindTurbin," MSc Thesis, Norwegian University of Science and Technology, 2012.
- [12] S.-H. Lee, J. Hong, Y. Kwon, Y.-S. Jo, and S. K. Baik, "Study on Homopolar Superconductivity Synchronous Motors for Ship Propulsion Applications," *IEEE Transactions on Applied Superconductivity*, vol. 18, no. 2, pp. 717–720, Jun. 2008. [Online]. Available: ieeexplore.ieee.org/xpl/articleDetails.jsp?arnumber=4523015
- [13] N. Maki, "Design study of high-temperature superconducting generators for wind power systems," *Journal of Physics: Conference Series*, vol. 97, p. 012155, Feb. 2008. [Online]. Available: <http://iopscience.iop.org/1742-6596/97/1/012155/>
- [14] S. Kalsi, B. Gamble, G. Snitchler, and S. Ige, "The status of HTS ship propulsion motor developments," in *2006 IEEE Power Engineering Society General Meeting*. IEEE, 2006, p. 5 pp. [Online]. Available: <http://ieeexplore.ieee.org/lpdocs/epic03/wrapper.htm?arnumber=1709643>
- [15] G. Snitchler, "Progress on high temperature superconductor propulsion motors and direct drive wind generators," *Power Electronics Conference (IPEC), 2010*, no. c, pp. 5–10, 2010. [Online]. Available: http://ieeexplore.ieee.org/xpls/abs_all.jsp?arnumber=5542327
- [16] A. B. Abrahamsen, N. Mijatovic, E. Seiler, T. Zirngibl, C. Træholt, P. B. Norgård, N. F. Pedersen, N. H. Andersen, and J. Ostergård, "Superconducting wind turbine generators," *Superconductor Science and Technology*, vol. 23, no. 3, p. 034019, Mar. 2010. [Online]. Available: <http://iopscience.iop.org/0953-2048/23/3/034019/>
- [17] F. Fair, W. Stautner, M. Douglass, R. Rajput-Ghoshal, M. Moscinski, P. Riley, D. Wagner, J. Kim, S. Hou, F. Lopez, K. Haran, J. Bray, T. Laskaris, J. Rochford, R. Duckworth, D. Wagner, J. Kim, S. Hou, F. Lopez, K. Haran, J. Bray, T. Laskaris, J. Rochford, and R. Duckworth, "Next Generation Drive Train - Superconductivity for Large-Scale Wind Turbines," in *Applied Superconductivity Conference*, no. 22, Portland, Oregon, 2012, pp. 1–29. [Online]. Available: <http://www.ewh.ieee.org/tc/csc/europe/newsforum/pdf/STP307.pdf>
- [18] P. J. Masson, "Wind Turbine Generators: Beyond the 10MW Frontier," in *Symposium on Superconducting Devices for Wind Energy Systems*, 2011, pp. 1–8.
- [19] H. Sung, G. Kim, K. Kim, S. Jung, and M. Park, "Practical Design of a 10 MW Class Superconducting Wind Power Generator Considering Weight Issue," no. 281, pp. 6–10, 2013. [Online]. Available: http://ieeexplore.ieee.org/xpls/abs_all.jsp?arnumber=6449292
- [20] B. Gamble, G. Snitchler, and T. MacDonald, "Full Power Test of a 36.5 MW HTS Propulsion Motor," *IEEE Transactions on Applied Superconductivity*, vol. 21, no. 3, pp. 1083–1088, Jun. 2011. [Online]. Available:

- <http://ieeexplore.ieee.org/lpdocs/epic03/wrapper.htm?arnumber=5676207>
- [21] S. Kalsi, "HTS ship propulsion motors," in *IEEE Power Engineering Society General Meeting, 2004.*, vol. 2. IEEE, 2004, pp. 2047–2048. [Online]. Available: <http://ieeexplore.ieee.org/lpdocs/epic03/wrapper.htm?arnumber=1373238>
 - [22] AMSC, "Concepts for High Power Wind Turbines - Introducing HTS Technology," in *World Green Energy Forum*, 2010. [Online]. Available: www.keei.re.kr/keei/download/seminar/101117/II101118_a01.pdf
 - [23] W. Stautner, R. Fair, K. Sivasubramaniam, K. Amm, J. Bray, E. T. Laskaris, K. Weeber, M. Douglass, L. Fulton, S. Hou, J. Kim, R. Longtin, M. Moscinski, J. Rochford, R. Rajput-Ghoshal, P. Riley, D. Wagner, and R. Duckworth, "Large Scale Superconducting Wind Turbine Cooling," *IEEE Transactions on Applied Superconductivity*, vol. 23, no. 3, p. 5200804, Jun. 2013. [Online]. Available: <http://ieeexplore.ieee.org/lpdocs/epic03/wrapper.htm?arnumber=6365243>
 - [24] Q. Chen, G. Liu, Z. Liu, and X. Li, "Design and Analysis of a New Fully Stator-HTS Motor," *IEEE Transactions on Applied Superconductivity*, vol. 24, no. 3, pp. 1–5, Jun. 2014. [Online]. Available: <http://ieeexplore.ieee.org/lpdocs/epic03/wrapper.htm?arnumber=6701206>
 - [25] O. Keysan and M. A. Mueller, "A Transverse Flux High-Temperature Superconducting Generator Topology for Large Direct Drive Wind Turbines," in *Superconductivity Centennial Conference*, vol. 01, 2011, pp. 1–6. [Online]. Available: <http://www.sciencedirect.com/science/article/pii/S1875389212019761>
 - [26] O. Keysan, D. Olczak, and M. A. Mueller, "A Modular Superconducting Generator for Offshore Wind Turbines," *Journal of Superconductivity and Novel Magnetism*, pp. 1–5, Dec. 2012. [Online]. Available: <http://www.springerlink.com/index/10.1007/s10948-012-1950-1>
 - [27] Vacuumschmelze, "VacoFlux (Soft Magnetic Cobalt-Iron-Alloys) Datasheet," Hanau, Germany, Tech. Rep., 2012. [Online]. Available: <http://www.vacuumschmelze.com/>
 - [28] J. W. R. Mebane and J. S. Sekhon, "Genetic Optimization Using Derivatives: The "rgenoud" Package for R," *Journal of Statistical Software*, vol. 42, no. 11, pp. 1–26, 2011. [Online]. Available: <http://www.jstatsoft.org/v42/i11/>
 - [29] D. Bang, "Design of Transverse Flux Permanent Magnet Machines for Large Direct-Drive Wind Turbines," PhD Dissertation, Delft University of Technology, 2010. [Online]. Available: http://repository.tudelft.nl/assets/uuid:c6867c53-fc10-468d-b6d7-082b7a052f4b/Final_thesis_DJBang_lowqlty.pdf
 - [30] A. B. Abrahamsen and B. B. Jensen, "Superconducting Direct Drive Wind Turbine Generators: Advantages and Challenges," in *Wind Energy Conversion Systems*, ser. Green Energy and Technology, S. Mueen, Ed. London: Springer London, 2012, ch. 3, pp. 53–80. [Online]. Available: <http://www.springerlink.com/index/10.1007/978-1-4471-2201-2>
 - [31] C. Simons, "Feasibility study of a superconducting helicopter electrical propulsion motor," MSc Thesis, Delft University of Technology, 2013.
 - [32] J. Ekin, *Experimental Techniques for Low-Temperature Measurements*, 1st ed. Oxford: Oxford University Press, 2006.
 - [33] S. Kalsi, "Cooling and Thermal Insulation Systems," in *Applications of High Temperature Superconductors to Electric Power Equipment*. John Wiley & Sons, Inc., 2011, ch. 3.
 - [34] Cryomech, "AL230 with CP950 - Cryorefrigerator Specification Sheet," Tech. Rep., 2007. [Online]. Available: http://cryomech.com/specificationsheet/AL230_ss.pdf
 - [35] G. Snitchler, B. Gamble, C. King, and P. Winn, "10 MW Class Superconductor Wind Turbine Generators," *IEEE Transactions on Applied Superconductivity*, vol. 21, no. 3, pp. 1089–1092, Jun. 2011. [Online]. Available: <http://ieeexplore.ieee.org/lpdocs/epic03/wrapper.htm?arnumber=5699957>
 - [36] Y. Terao, M. Sekino, and H. Ohsaki, "Electromagnetic Design of 10 MW Class Fully Superconducting Wind Turbine Generators," *IEEE Transactions on Applied Superconductivity*, vol. 22, no. 3, p. 5201904, Jun. 2012. [Online]. Available: <http://ieeexplore.ieee.org/lpdocs/epic03/wrapper.htm?arnumber=6092460>

- [37] N. Kim, G. Kim, K. Kim, M. Park, I. Yu, S. Lee, E. Song, and T. Kim, "Comparative Analysis of 10 MW Class Geared and Gearless Type Superconducting Synchronous Generators for a Wind Power Generation System," *IEEE Transactions on Applied Superconductivity*, vol. 22, no. 3, pp. 5 202 004–5 202 004, Jun. 2012. [Online]. Available: http://ieeexplore.ieee.org/xpls/abs_all.jsp?arnumber=6095601
- [38] M. R. Quddes, M. Sekino, H. Ohsaki, N. Kashima, and S. Nagaya, "Electromagnetic Design Study of Transverse Flux Enhanced Type Superconducting Wind Turbine Generators," *IEEE Transactions on Applied Superconductivity*, vol. 21, no. 3, pp. 1101–1104, Jun. 2011. [Online]. Available: <http://ieeexplore.ieee.org/lpdocs/epic03/wrapper.htm?arnumber=5692864>